

## Dependence of Optical Matrix Elements on the Boundary Conditions of the Continuum States in Quantum Wells

Y. R. Jang and K. H. Yoo\*

*Department of Physics and Research Institute for Basic Sciences, Kyung Hee University, Seoul 130-701, KOREA*

L. R. Ram-Mohan

*Departments of Physics, Electrical and Computer Engineering, Worcester Polytechnic Institute, Worcester, Massachusetts 01609, USA*

(Received February 14, 2005 : revised May 26, 2005)

Unlike for the bound states, several different boundary conditions are used for the continuum states above the barrier in semiconductor quantum wells. We employed three boundary conditions, infinite potential barrier boundary condition, periodic boundary condition and scattering boundary condition, and calculated the local number of states, wavefunctions and optical matrix elements for the symmetric and asymmetric quantum wells. We discussed how these quantities are related in the three boundary conditions. We argue that the scattering boundary condition has several advantages over the other two cases. These results would be useful in understanding quantum well lasers and detectors involving continuum states.

OCIS codes : 000.1600, 040.4200, 040.5160, 140.5960, 230.5590

### I. INTRODUCTION

In most cases, physical properties of interest in quantum wells (QWs) are dominated by the ground state, and the ground state is a bound state. However, the continuum states are important in understanding some quantum well devices such as quantum well lasers operating at high temperature [1, 2] and quantum well infrared detectors utilizing bound-to-continuum transitions [3, 4].

Only one boundary condition is used in describing bound states of quantum wells; the envelope function and its derivative go to zero far away from the well. On the contrary, several different boundary conditions are used in describing continuum states. But studies comparing the different boundary conditions and their results in detail are rare [5].

In this paper, we chose three different boundary conditions for continuum states; infinite potential barrier boundary condition (IPBC) [1, 6-9], periodic boundary condition (PRBC) [9] and scattering boundary condition (SCBC) [10-12]. We reviewed these boundary conditions and applied them to symmetric and asymmetric quantum wells. We numerically calculated the local number of states [9, 13], wavefunctions and optical matrix elements,

and discussed how these quantities are related in the three boundary conditions. We found that the scattering boundary condition has several advantages over the other two boundary conditions.

### II. THREE BOUNDARY CONDITIONS

We consider a quantum well schematically shown in Fig. 1. In the one-band envelope function picture [14], the one dimensional Schrödinger's equation is written as

$$-\frac{\hbar^2}{2} \frac{d}{dz} \left( \frac{1}{m^*(z)} \frac{df(z)}{dz} \right) + V(z)f(z) = Ef(z). \quad (1)$$

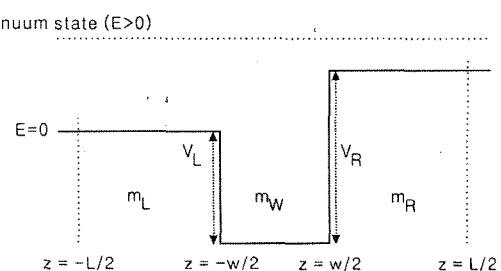


FIG. 1. Schematic diagram of a quantum well.

The origin of the  $z$ -coordinate is chosen to be the center of the well as shown in Fig. 1. In Eq. (1),  $f(z)$  is the envelope function,  $m^*(z)$  is the effective mass in each layer given by

$$\begin{aligned} m^*(z) &= m_L, \quad \text{if } z < -w/2, \\ &= m_W, \quad \text{if } -w/2 < z < w/2, \\ &= m_R, \quad \text{if } z > w/2, \end{aligned} \quad (2)$$

and  $V(z)$  is the potential due to band offset given by

$$\begin{aligned} V(z) &= 0, & \text{if } z < -w/2, \\ &= -V_L, & \text{if } -w/2 < z < w/2, \\ &= -V_L + V_R, & \text{if } z > w/2. \end{aligned} \quad (3)$$

Note that we measure the energy from the top of the left barrier. We assume  $V_R \geq V_L$  without loss of generality.

Since the potential in each region is constant, the wavefunction can be written as

$$\begin{aligned} f_L(z) &= a_1 \exp(ik_L z) + b_1 \exp(-ik_L z), & \text{for } z < -w/2, \\ f_W(z) &= a_2 \exp(ik_W z) + b_2 \exp(-ik_W z), & \text{for } -w/2 < z < w/2, \\ f_R(z) &= a_3 \exp(ik_R z) + b_3 \exp(-ik_R z), & \text{for } z > w/2, \end{aligned} \quad (4)$$

where

$$\begin{aligned} k_L &= \sqrt{2m_L E / \hbar^2}, \\ k_W &= \sqrt{2m_W (E + V_L) / \hbar^2}, \\ k_R &= \sqrt{2m_R (E + V_L - V_R) / \hbar^2}. \end{aligned} \quad (5)$$

For a continuum state ( $E > 0$ ),  $k_L$  and  $k_W$  are real numbers, while  $k_R$  can be pure imaginary if  $E < (V_R - V_L)$ .

We require that the wavefunction and probability current be continuous across the interface, and get the following four equations.

$$\begin{aligned} f_L(-w/2) &= f_W(-w/2), \\ \frac{1}{m_L} \frac{df_L}{dz} \Big|_{(-w/2)} &= \frac{1}{m_W} \frac{df_W}{dz} \Big|_{(-w/2)}, \\ f_W(w/2) &= f_R(w/2), \\ \frac{1}{m_W} \frac{df_W}{dz} \Big|_{(w/2)} &= \frac{1}{m_R} \frac{df_R}{dz} \Big|_{(w/2)}. \end{aligned} \quad (6)$$

These interface conditions provide 4 equations to solve 6 unknowns in Eq. (4). The other 2 equations are supplied by the boundary conditions far away from the well.

### 1. Infinite potential barrier boundary condition (IPBC) [1,6-9]

In this IPBC, we place infinite potential barriers at  $z = \pm L/2$  which are assumed to be far enough from the

well. The wavefunction becomes zero at these positions.

$$\begin{aligned} f_L(-L/2) &= 0, \\ f_R(L/2) &= 0. \end{aligned} \quad (7)$$

These 2 equations together with 4 equations in Eq. (6) forms an eigenvalue equation, which gives discrete eigenvalues  $E$  and corresponding unnormalized wavefunctions, i.e, the ratios among the 6 unknowns  $a_1$ ,  $b_1$ , ..., and  $b_3$  in Eq. (4). The normalization of the wavefunction is given by

$$\int_{-L/2}^{L/2} |f(z)|^2 dz = 1. \quad (8)$$

With this normalization, the wavefunction has a dimension of  $1/\sqrt{\text{length}}$ .

### 2. Periodic boundary condition (PRBC) [9]

Again an arbitrary boundary  $z = \pm L/2$  is introduced, and the wavefunction is assumed to be periodic in  $[-L/2, L/2]$ .

$$\begin{aligned} f_L(-L/2) &= f_R(L/2), \\ \frac{1}{m_L} \frac{df_L}{dz} \Big|_{(-L/2)} &= \frac{1}{m_R} \frac{df_R}{dz} \Big|_{(L/2)}. \end{aligned} \quad (9)$$

As in IPBC case, the 6 equations in Eq. (6) and Eq. (9) form an eigenvalue equation, and the wavefunction is normalized by Eq. (8).

### 3. Scattering boundary condition (SCBC) [10-12]

In this SCBC, a particle is incident either from the left or from the right. For a wave incident from the left, the amplitude  $a_1$  and energy  $E$  of the incoming wave are assumed to be given and  $b_3$  is set to zero. Then 4 equations in Eq. (6) determines 4 unknowns  $b_1$  (usually called reflection coefficient),  $a_2$ ,  $b_2$  and  $a_3$  (transmission coefficient). In order to normalize the wavefunction to represent one particle,  $a_1$  should be set to  $1/\sqrt{2\pi}$  [12].

$$a_1 = 1/\sqrt{2\pi}. \quad (10)$$

The wavefunction in SCBC is dimensionless in contrast with the other two cases where the wavefunction has a dimension of  $1/\sqrt{\text{length}}$ .

Unlike the other two BCs, in SCBC case, we do not need to introduce an arbitrary boundary  $z = \pm L/2$ , and we have a truly continuous energy spectrum. The wave incident from the right can be constructed in a similar way if  $E > (V_R - V_L)$ .

### III. NUMERICAL RESULTS AND DISCUSSIONS

It is commonly believed that the 3 BCs should give the same physical results if  $L$  is sufficiently large. We numerically calculated the local number of states [9, 13], wavefunctions and optical matrix elements as functions of  $L$  and compared the results.

For a numerical calculation, we considered a symmetric  $\text{Al}_{0.2}\text{Ga}_{0.8}\text{As}/\text{GaAs}/\text{Al}_{0.2}\text{Ga}_{0.8}\text{As}$  QW and an asymmetric  $\text{Al}_{0.2}\text{Ga}_{0.8}\text{As}/\text{GaAs}/\text{Al}_{0.35}\text{Ga}_{0.65}\text{As}$  QW. The input parameters were taken from Ref. [15] and summarized in Table 1. For the parts of the local number of states and wavefunctions, the conduction band parameters were used.

#### 1. Local number of states (LNOS)

The local number of states  $N_W(E)$  is defined as the number of states whose energy is less than  $E$  weighted by the probability that the electron is in the well. In IPBC and PRBC, it can be written as

$$N_W(E) = \sum_{i(E_i \leq E)} \int_{-w/2}^{w/2} dz |f_i(z)|^2. \quad (11)$$

The index  $i$  runs over the discrete eigenstates. In SCBC, it is given by

$$N_W(E) = \int_0^{\sqrt{2m_L E/\hbar^2}} dk_L \int_{-w/2}^{w/2} dz |f_{k_L}(z)|^2 + \int_0^{\sqrt{2m_R(E - V_R + V_L)/\hbar^2}} dk_R \int_{-w/2}^{w/2} dz |f_{k_R}(z)|^2. \quad (12)$$

In Eq. (12), the wavefunction for the wave incident from the left (right) is labelled by  $k_L$  ( $k_R$ ), and the wave-

vectors  $k_L$  and  $k_R$  are functions of  $E$  given by Eq. (5).

In Fig. 2, we compare LNOS of the symmetric 100 Å  $\text{Al}_{0.2}\text{Ga}_{0.8}\text{As}/\text{GaAs}/\text{Al}_{0.2}\text{Ga}_{0.8}\text{As}$  QW for three BCs for  $L = 2w$  (Fig. 2 (a)) and  $L = 15w$  (Fig. 2 (b)). The discrete LNOS in IPBC/PRBC and continuous LNOS in SCBC are clearly shown. Since SCBC does not use  $L$ , it gives the same curve in Fig. 2 (a) and (b). As  $L$  increases, LNOS of IPBC/PRBC approaches that of SCBC, as expected. In principle this agreement becomes

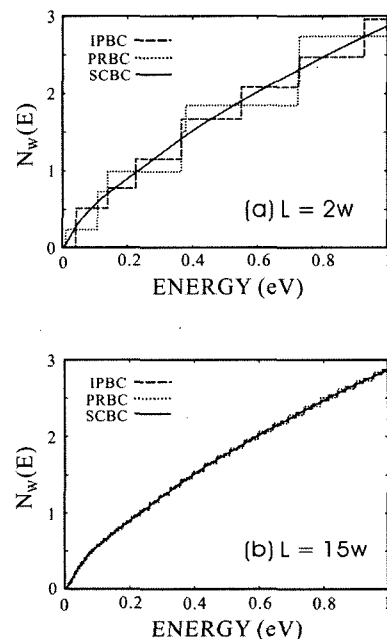


FIG. 2. Local number of states of the symmetric 100 Å  $\text{Al}_{0.2}\text{Ga}_{0.8}\text{As}/\text{GaAs}/\text{Al}_{0.2}\text{Ga}_{0.8}\text{As}$  QW for three BCs; (a) for  $L = 2w$  and (b) for  $L = 15w$ .

TABLE 1. Band parameters used in this calculation.

parameter	GaAs	$\text{Al}_{0.2}\text{Ga}_{0.8}\text{As}$	$\text{Al}_{0.35}\text{Ga}_{0.65}\text{As}$
<i>conduction band</i>			
effective mass ( $m_0$ )	0.067	0.0812	0.0908
band offset <sup>†</sup> (eV)	0	0.1883	0.2919
<i>heavy-hole band</i>			
effective mass ( $m_0$ )	0.3687	0.3497	0.3845
band offset <sup>†</sup> (eV)	0	-0.1060	-0.1855
<i>interband interaction</i>			
$E_p$ (eV)	21.6250	22.5211	20.9529

<sup>†</sup> with respect to GaAs.

better for larger  $L$ , but in practice we encounter a numerical problem for large  $L$ . For large  $L$ , the eigenvalues are close each other, and a very small numerical error in determining an eigenvalue can lead to a bad wavefunction which in turn gives a wrong LNOS in IPBC/PRBC.

Fig. 3 is for the case of asymmetric  $\text{Al}_{0.2}\text{Ga}_{0.8}\text{As}/\text{GaAs}/\text{Al}_{0.35}\text{Ga}_{0.65}\text{As}$  QW in which the right barrier is higher than the left barrier by 0.1036 eV. In SCBC, only incident-from-the-left states exist for  $E < 0.1036$  eV, while incident-from-the-right states also exist for higher energies. Again, LNOS of IPBC/PRBC approaches that of SCBC as  $L$  increases.

## 2. Wavefunctions

In Fig. 4 (a) and (b), we compare the square of the first continuum state wavefunction in IPBC and PRBC for the symmetric QW at  $L = 15w$ . The wavefunctions have two nodes because the 1st continuum state is the 3rd state if we count the two bound states. The magnitude of the continuum state wavefunction is larger in the barrier region in contrast to the bound state wavefunction which is larger in the well region. The wavefunction in IPBC goes to zero at  $z = \pm L/2$  as the boundary conditions in Eq. (7) require, while no such behavior occurs in PRBC. The overall shape of the wavefunction is quite different in the two cases, even though LNOSs in the two cases are close at  $L = 15w$ .

There is no first continuum state in the SCBC case

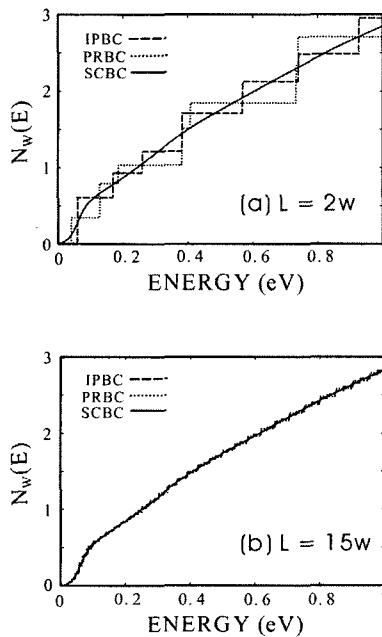


FIG. 3. Local number of states of the asymmetric 100 Å  $\text{Al}_{0.2}\text{Ga}_{0.8}\text{As}/\text{GaAs}/\text{Al}_{0.35}\text{Ga}_{0.65}\text{As}$  QW for three BCs; (a) for  $L = 2w$  and (b) for  $L = 15w$ .

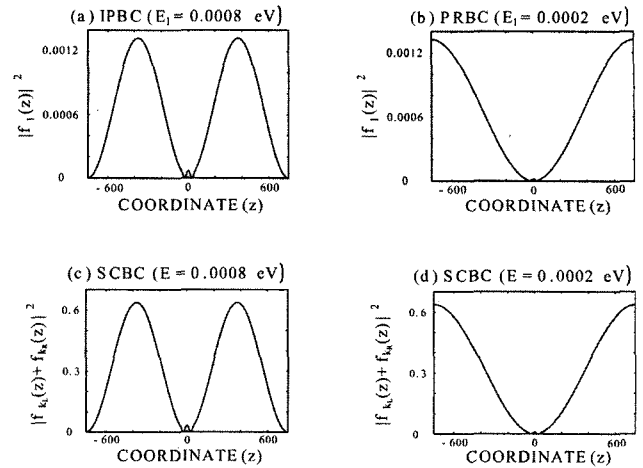


FIG. 4. The first continuum state wavefunctions in IPBC and PRBC and corresponding wavefunctions in SCBC for the symmetric QW at  $L = 15w$ .

since the energy spectrum is continuous. We can construct the wavefunction in IPBC or PRBC by linear combination of the SCBC wavefunctions

$$f_i = N[f_{k_L(E)} + bf_{k_R(E)}], \quad (13)$$

where  $N$  is determined by normalization. We can choose  $E$  and  $b$  to satisfy the boundary conditions (Eq. (7) or Eq. (9)) of IPBC or PRBC. For the first continuum state,  $E$  is the first continuum state eigenenergy in either IPBC or PRBC (0.000816 and 0.000204 eV, respectively), and the phase factor  $b$  is 1. In general,  $b$  is 1 for even states and -1 for odd states for a symmetric QW. Fig. 4 (c) and (d) are SCBC wavefunctions  $f_{k_L(E)} + bf_{k_R(E)}$  constructed in such a way, and we can see they are same as IPBC or PRBC wavefunction except for the normalization factor.

In the asymmetric QW, some states in IPBC or PRBC may be below the right barrier, and there are no corresponding incident-from-the-right states. In this case, we cannot construct IPBC or PRBC wavefunction from SCBC wavefunctions; if there is no  $f_{k_R(E)}$  term in the expression  $N[f_{k_L(E)} + bf_{k_R(E)}]$ , we have only one parameter  $E$  and cannot satisfy BCs at two ends. If the continuum state eigenenergies are higher than the right barrier in the asymmetric QW, we can construct the wavefunction of IPBC or PRBC from the SCBC wavefunctions in the form of  $N[f_{k_L(E)} + bf_{k_R(E)}]$ . Unlike the symmetric QW, the factor  $b$  is in general a complex number.

## 3. Optical matrix elements

The interband optical matrix element between a heavy hole state and an electron state can be written as [14]

$$M = |\langle f_e u_e | \hat{\epsilon} \cdot \vec{p} | f_{hh} u_{hh} \rangle|^2, \quad (14)$$

where  $f$  and  $u$  are the envelope function and the periodic part of the Bloch state, respectively. If we consider the transverse electric polarization ( $\hat{\epsilon} = \hat{x}$ ), we have

$$\langle u_e | p_x | u_{hh} \rangle = \langle S | p_x | \frac{1}{\sqrt{2}}(X + iY) \rangle = \frac{1}{\sqrt{2}}P, \quad (15)$$

where the interband momentum matrix element  $P = \langle S | p_x | X \rangle$  is related to the interband interaction energy  $E_p$  by

$$E_p = \frac{2P^2}{m_0}. \quad (16)$$

We consider only the transitions from the bound ground heavy-hole state to the continuum electron states. In IPBC or PRBC where the continuum electron states are discrete and labelled by  $i$ , the matrix element can be written

$$M_i = \frac{1}{2} |\langle f_i | P | f_{hh1} \rangle|^2. \quad (17)$$

In SCBC the corresponding equation for the incident-from-the-left state is

$$M_{k_L} = \frac{1}{2} |\langle f_{k_L} | P | f_{hh1} \rangle|^2. \quad (18)$$

with a similar equation for the incident-from-the-right state. The total matrix element in SCBC is given by

$$M(E) = M_{k_L(E)} + M_{k_R(E)}. \quad (19)$$

For a numerical example, we plotted  $M_i$  versus  $E_i$  for IPBC/PRBC and  $M(E)$  for SCBC for a symmetric QW with  $L = 15w$  in Fig. 5 (a). First of all,  $M_i$  and  $M(E)$  do not have the same unit because  $f_i$  and  $f_{k_L}$  have different units. In Fig. 5 (a),  $M_i$  is drawn to the scale of  $\text{eV}^2/c^2$  and  $M(E)$  in  $\text{eV}^2 \text{\AA}/c^2$  is scaled arbitrarily for easy comparison with  $M_i$ . Another point is that  $M_i$  has an interference term between  $f_{k_L}$  and  $f_{k_R}$  since  $f_i$  in Eq. (17) can be written in the form  $N[f_{k_L(E)} + bf_{k_R(E)}]$  while there is no such interference in  $M(E)$  in Eq. (19). This interference is evident for odd-parity conduction states for which  $M_i = 0$ , as can be seen in Fig. 5 (a). However, for the even-parity states,  $M_i$  and  $M(E)$  have a similar shape as a function of energy.  $M(E)$  have peaks that are related to the virtual states in the conduction band.

We may think that the continuous matrix element in SCBC is redistributed into discrete ones in IPBC or PRBC due to the boundary conditions at  $z = \pm L/2$  and the sum of matrix elements should be the same in the three cases. Therefore we introduce a ‘‘cumulative’’ matrix element as

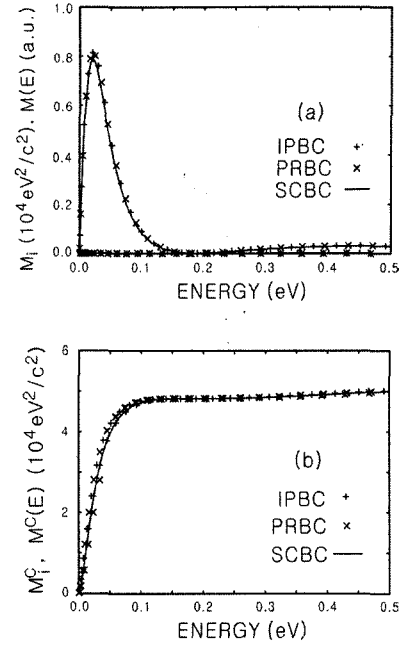


FIG. 5. (a) Optical matrix elements and (b) cumulative matrix elements as a function of conduction band energy for the symmetric QW at  $L = 15w$ .

$$M_i^C = \sum_{j(E_j \leq E_i)} M_j \quad (20)$$

for IPBC/PRBC, and

$$M^C(E) = \int_0^{\sqrt{2m_L E/\hbar^2}} dk_L M_{k_L} + \int_0^{\sqrt{2m_R(E - V_n + V_L)/\hbar^2}} dk_R M_{k_R} \quad (21)$$

for SCBC. If  $f_{hh1}$  is constant in the well and zero outside the well, these ‘‘cumulative’’ matrix elements are proportional to the local number of states defined in Eq. (11) and Eq. (12). These  $M_i^C$  and  $M^C(E)$  have the same unit, and they are compared in Fig. 5 (b). The cumulative matrix elements agree well for the three boundary conditions if  $L$  is large enough so that there are enough number of states in the region where  $M(E)$  varies significantly. This is true of the asymmetric QW case.

It seems that IPBC is the most frequently used boundary condition to describe the continuum states of QW [1, 6-9]. However, we suggest that SCBC be the best choice. SCBC does not need to introduce an arbitrary parameter  $L$ . It contains almost all the informations that IPBC or PRBC gives in the sense that the wavefunction in IPBC or PRBC can be constructed from those in SCBC. Numerically, IPBC and PRBC yield an eigenvalue problem, and a very small numerical error in eigenvalue leads to a bad wavefunction, especially at large  $L$ . No such numerical instability occurs in the coupled algebraic equations of SCBC.

#### IV. CONCLUSION

We have reviewed three most frequently used boundary conditions, infinite potential barrier boundary condition, periodic boundary condition and scattering boundary condition, to describe the continuum states of quantum wells. IPBC and PRBC introduce an arbitrary parameter  $L$ . IPBC and PRBC yield an eigenvalue problem, which can be numerically unstable at large  $L$ , while SCBC yields an ordinary algebraic equation. The wavefunction in IPBC and PRBC has dimension of  $1/\sqrt{\text{length}}$  while that of SCBC is dimensionless. In most cases, the wavefunctions in IPBC and PRBC can be constructed from those of SCBC. The continuous physical quantities such as optical matrix element in SCBC are redistributed into discrete ones in IPBC and PRBC, and the quantities integrated in energy such as cumulative matrix elements should be compared. The local number of states and the cumulative matrix element in the three boundary conditions agree each other as  $L$  increases. We suggest that SCBC be better than the other two in several respects. These results would be useful in understanding quantum well lasers and detectors involving continuum states.

#### ACKNOWLEDGMENTS

This research was supported by the Kyung Hee University Research Fund in 2003.

\*Corresponding author : khyoo@khu.ac.kr

#### REFERENCES

- [1] S. T. Yen and C.-P. Lee, "Theoretical analysis of 630 nm band GaInP-AlGaInP strained quantum-well lasers considering continuum states," *IEEE J. Quantum Electron.*, vol. 33, no. 3, pp. 443-456, 1997.
- [2] H. Hirayama, Y. Miyaki and M. Asada, "Analysis of current injection efficiency of separate-confinement-heterostructure quantum-film lasers," *IEEE J. Quantum Electron.*, vol. 38, no. 1, pp. 68-74, 1992.
- [3] B. F. Levine, C. G. Bethea, K. K. Choi, J. Walker and R. J. Malik, "Bound-to-extended state absorption GaAs superlattice transport infrared detectors," *J. Appl. Phys.*, vol. 64, no. 3, pp. 1591-1593, 1988.
- [4] B. F. Levine, G. Hasnain, C. G. Bethea and N. Chand, "Broadband 8-12  $\mu\text{m}$  high-sensitivity GaAs quantum well infrared photodetector," *Appl. Phys. Lett.*, vol. 54, no. 26, pp. 2704-2706, 1989.
- [5] Y. Fu, "Boundary conditions of continuum states in characterizing photocurrent of GaAs/AlGaAs quantum well infrared photodetector," *Superlattices and Microstructures*, vol. 30, no. 2, pp. 69-74, 2001.
- [6] J. D. Bruno and T. B. Bahder, "Local density of states in double-barrier resonant-tunneling structures, II. Finite-width barriers," *Phys. Rev. B*, vol. 39, no. 6, pp. 3659-3663, 1989.
- [7] S. Fafard, "Energy levels in quantum wells with capping barrier layer of finite size: bound states and oscillatory behavior of the continuum states," *Phys. Rev. B*, vol. 46, no. 8, pp. 4659-4666, 1992.
- [8] Rusli, T. C. Chong and S. J. Chua, "Theoretical analysis of bound-to-continuum state infrared absorption in GaAs/Al $x$ Ga $1-x$ As quantum well structures," *Jpn. J. Appl. Phys.*, vol. 32, part 1, no. 5A, pp. 1998-2004, 1993.
- [9] T. B. Bahder, J. D. Bruno, R. G. Hay and C. A. Morrison, "Local density of states in double-barrier resonant-tunneling structures," *Phys. Rev. B*, vol. 37, no. 11, pp. 6256-6261, 1988.
- [10] G. Iannaccone, "General relation between density of states and dwell times in mesoscopic systems," *Phys. Rev. B*, vol. 51, no. 7, pp. 4727-4729, 1995.
- [11] L. I. Schiff, *Quantum Mechanics* (McGraw-Hill, New York, USA, 1949), pp. 41-103.
- [12] R. Shankar, *Principles of Quantum Mechanics*, 2nd ed. (Plenum, New York, USA, 1994), pp. 167-175.
- [13] W. Trzeciakowski and M. Gurioli, "Electric-field effects in semiconductor quantum wells," *Phys. Rev. B*, vol. 44, no. 8, pp. 3880-3890, 1991.
- [14] G. Bastard, *Wave Mechanics Applied to Semiconductor Heterostructures* (Les Editions de Physique, Les Ulis, France, 1988), pp. 63-113 and pp. 237-257.
- [15] I. Vurgaftman, J. R. Meyer, and L. R. Ram-Mohan, "Band parameters for III-V compound semiconductors and their alloys," *J. Appl. Phys.*, vol. 89, no. 11, pp. 5815-5875, 2001.